

1 Ammonium removal by liquid-liquid membrane 2 contactors in water purification process for hydrogen 3 production

4 Edxon Licon^{1*}, Mònica Reig¹, Pilar Villanova¹, Cesar Valderrama¹, Oriol Gibert^{1,2}, José
5 Luis Cortina^{1,2}

6 ¹Chemical Engineering Dept. UPC-Barcelona TECH, Av. Diagonal 647, 08028
7 Barcelona, Spain,

8 ²CETAQUA Carretera d'Esplugues, 75, 08940 Cornellà de Llobregat, Spain

9
10 *Corresponding author: Edxon Eduardo Licon Bernal

11 Email: edxon.eduardo.licon@upc.edu; Phone: (+34) 934016997

12
13 Mònica Reig, monica.reig@upc.edu; (+34) 934016997
14 Pilar Villanova, pilar.villanova@gmail.com; (+34) 934016997
15 Cesar Valderrama, cesar.alberto.valderrama@upc.edu; (+34) 934015877
16 Oriol Gibert, oriol.gibert@upc.edu; (+34) 934011818
17 José Luis Cortina, jose.luis.cortina@upc.edu; (+34) 934016570

18 Abstract

19 In this work a liquid-liquid membrane contactor (LLMC) was evaluated to remove
20 ammonia traces from water used for hydrogen production by electrolysis. Three
21 operational parameters were evaluated: the feed flow rate, the initial ammonia
22 concentration in the water stream and the pH of solution. Synthetic aqueous solutions
23 with ammonium concentration of 5 to 25 mg·L⁻¹ and a sulfuric acid solution (pH=2)
24 were supplied to the LLMC in countercurrent and open loop configuration with flow
25 rates between 2.72×10^{-6} and 22.6×10^{-6} m³·s⁻¹ and the pH values of the solution with
26 ammonium between 8 and 11. A 2D numerical model was developed considering
27 advection-diffusion equation inside a single fiber of the lumen with fully developed
28 laminar flow and liquid gas equilibrium in the membrane-solution interface. Predictions
29 of the model were then validated against experimental data which were found to be in
30 good agreement. According to both, experimental data and numerical predictions, the
31 hollow fiber membrane contactor technology is a suitable alternative to remove
32 ammonium from water and to feed the membrane distillation unit in order to fulfil water
33 quality requirements for electrolysis-based hydrogen production.

34 **Keywords:** Ammonium removal; Membrane contactors; Open loop configuration;
35 Numerical simulation;

1. Introduction

Hydrogen is considered a clean energy source since only water vapor is obtained during its combustion. However, its production from water by electrolysis is limited by water quality requirements in terms of ionic conductivity. This study is part of a project which had the purpose of reducing the water footprint of urban water treatment plants by coupling hydrogen generating stations. This hydrogen would be produced by electrolysis of water produced by the treatment plant. As essential requirements, the water introduced to the electrolyser should have a low concentration of suspended solids and low conductivity [1]. For this purpose, ultrafiltration and membrane distillation units were initially installed. However, the presence of ammonia was detected in the feeding water [2].

Due to its ionic nature, the present ammonium contributes to high conductivity of the solution, decreasing the efficacy of the electrolyser even when ammonia concentration was very low (5-15 mg·L⁻¹). In turn, the fact that ammonia is a volatile compound makes difficult its elimination when water is purified using direct contact membrane distillation to remove salts and other compounds evaporating the water [3].

Ammonium is converted into ammonia at pH values higher than the pKa=9.3 at 298K and its equilibrium is shown in Equation 1.



Due to this characteristic, a membrane contactor with hydrophobic membrane was proposed to remove the ammonium traces in the water. A membrane contactor is a device in which a transfer of mass from gas to liquid, liquid to liquid or liquid to gas is produced without dispersion of one of the phases into the other [4]. For the liquid-liquid mode, the transfer of the molecules through the walls of the hollow membranes is produced by the existence of a concentration gradient between the solution inside (lumen) and the solution flowing outside the fiber (shell). The membrane enhances the transfer of molecules through the pores of the fibers and provides direct contact between the removed gas and both fluids, avoiding the mixing between the two resulting solutions [5].

The removal of ammonia by membrane distillation has been studied previously. For instance, Xie *et. al* [6] studied the removal of wastewater containing low levels of

1 ammonia (100 mg/L) through simulation of experiments with sweep gas membrane
2 distillation at pH 11.5. Ding et al [7], compared the separation performance of three
3 kinds of membrane distillation direct contact membrane distillation, vacuum membrane
4 distillation and sweeping gas membrane distillation used in the removal of ammonia
5 from water. They determined key factors that may affect the separation processes, such
6 as the membrane characteristics, the feed temperature, feed and permeate velocity, and
7 the initial concentration and pH of the feed solution. Bourawi et al. [8], investigated the
8 applicability of vacuum membrane distillation for ammonia removal from its aqueous
9 solutions using membrane distillation was also studied by Bourawi et al [8] obtaining
10 removal efficiencies higher than 90%.

11 On the other hand, the removal mechanism of ammonium using hollow fiber membrane
12 contactors have been studied in the last years and a variety of mathematical models can
13 be found. Semmens et al. [9] studied the nonlinear relation on the resistances related to
14 the transport of ammonia. Wickramasinghe et al. [10] demonstrated that the separation
15 efficiency was controlled by the resistance in the lumen side and determined the mass
16 transfer coefficients of ammonia using different configurations. Tan et al. [11] modeled
17 the removal of ammonia and compared its results with experimental work done with
18 Polyvinylidene fluoride (PVDF) membrane contactors, incorporating the resistance in
19 the feed and membrane phases. Ashrafizadeh and Khorasani [4] studied the influence of
20 different parameters, such as inlet feed flow, initial concentration, temperature or pH, on
21 the ammonia removal efficiency and optimized the process for a commercial membrane
22 contactor. Mandowara and Bhattacharya [12] developed a 2D mathematical model for
23 polypropylene (PP) membrane contactors incorporating the effect of pore diffusion,
24 mass transfer resistance was taken into account. Agrahari et al. [13] developed a model
25 incorporating molecular and Knudsen diffusion effects as well as the rates of adsorption
26 and desorption of ammonia molecules to and from the walls of the pores during the
27 transport through the membrane. More recently, Rezakazemi et al. [14] used a finite
28 element approach to solve a 2D diffusion model to predict the unsteady state of
29 ammonia transport. Nosratina et al., [15], included the continuity equation for the
30 transport of ammonia inside the membrane pores, which was considered to be
31 controlled by diffusion. Most of the past work has been done for close-loop
32 configuration and only in a previous work [5], Mandowara and Bhattacharya studied the
33 open loop case with liquid-gas configuration working under vacuum conditions in the
34 shell side of the contactor. Accordingly, in order to understand the phenomena

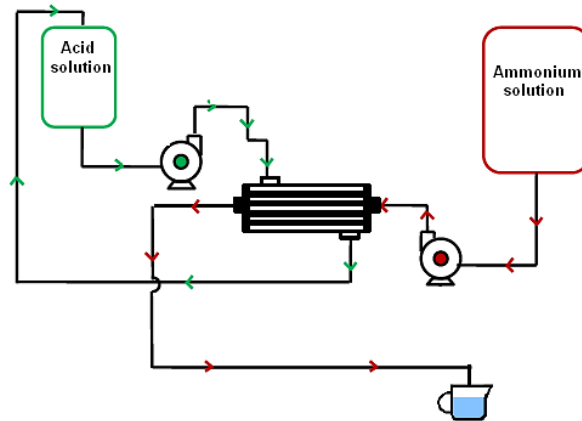
1 occurring in the separation process studied here, it is necessary to develop a model where
2 the open loop liquid-liquid configuration can be described considering all contributions
3 made by the authors previously mentioned. This configuration is more reliable in terms
4 of the water hydrolysis process since it is desired to operate in continuous regimen at
5 pilot plant scale.

6 The present work is a feasibility study on the use of liquid-liquid membrane contactors
7 in open loop for removing traces of ammonia from water, in order to fulfill the adequate
8 conditions for the production of hydrogen by electrolysis. The dependence of the
9 removal efficiency on the initial concentration, pH and flow rate will be evaluated
10 experimentally and numerical simulations will be used to describe the transport
11 phenomena in the LLMC. It will be demonstrated that the use of open-loop
12 configuration is possible when using a given number of membrane contactors in series.

13 **2. Material and methods**

14 **2.1 Experimental description and operation**

15 Experiments were carried out by using the set-up shown in Figure 1. It consisted of the
16 LLMC module, two peristaltic pumps and two polypropylene tanks, one for the
17 ammonium chloride solutions and the other for the sulfuric acid solution at pH=2 (0.02
18 M). The volume of the acid solution was 25 liters. All test components were connected
19 by clear PVC flexible tubes. The contactor module used was a Liqui-Cel 2.5 x 8" Extra
20 Flow X30HF (Celgard, USA). The pH of the ammonium solution was increased by
21 adding sodium hydroxide and the solution was buffered with sodium tetraborate. All
22 reagents used were of analysis quality (PA-ACS-ISO reagent, PANREAC). The
23 ammonia concentration at the outlet of the module was determined during the
24 experiments with a selective ammonia electrode (HACH 51927) with a sampling time
25 of 5 minutes until the steady state was reached. The values reported are those obtained
26 in the steady state.



1

2 Figure 1. Experimental setup for the study of ammonium removal in open-loop
 3 configuration with a LLMC.

4 The experiments were divided in three different groups in order to evaluate the
 5 performance of the process under several values of the flow rate (Q), pH of the
 6 ammonium solution and its initial ammonium concentration (C_0). All the values are
 7 listed in Table 1.

8 Table 1. Values of the parameters studied for the three different groups of experiments.

Experiment group	$Q \times 10^6 \text{ (m}^3 \cdot \text{s}^{-1}\text{)}$	pH	$C_0 \text{ (mg} \cdot \text{L}^{-1}\text{)}$
Flow rate	2.72	10	15
	3.48		
	6.12		
	8.86		
	13.3		
	22.6		
pH	3.48	8	15
		8,5	
		9	
		9,5	
		10	
Initial concentration	3.48	10	5
			10
			15
			20
			25
			35

9

2.2 Theory and model development

In aqueous solution, ammonium and ammonia are present depending on the pH equilibrium. This is an unsteady-state process in which the transport is governed by axial diffusion, radial diffusion, and convection in the lumen side. A three-step transport may be considered to occur sequentially during the ammonia removal (see Figure 2). The first step is radial diffusion to the internal surface of the hollow fiber. The second step is the diffusion of ammonia inside the pore. Finally, ammonia in gaseous form reaches the pore exit of the hydrophobic membrane and instantaneously reacts with the acid solution. No reaction zone is formed due to the high solubility of the ammonia in acid solutions; it reacts only at the interface. Given the above considerations, the numerical model is based on the following assumptions [12]:

1. Isothermal operation;
2. Fully developed parabolic profile in the lumen side;
3. No pore blockages and pores are filled with air;
4. Feed and extract volumes (and hence tank volumes) are large compared to that of the hollow-fibre module;

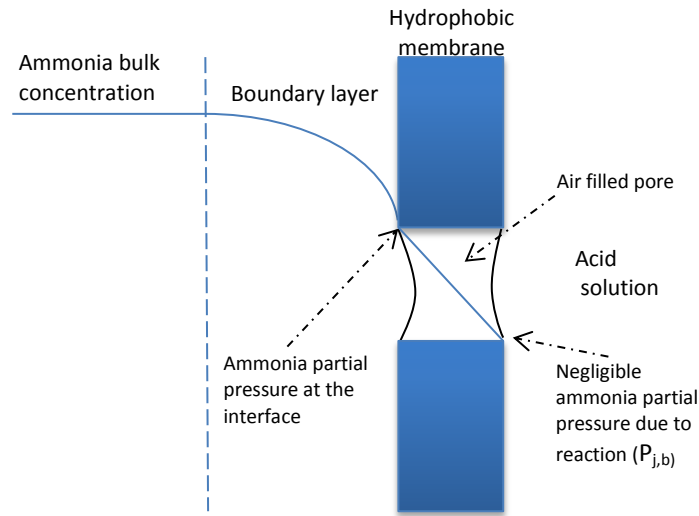


Figure 2. Ammonia partial pressure profile when it moves from a liquid phase towards an acid solution through a hydrophobic membrane.

Let N_j be the molar flux of species j being transferred then at steady state, molar flux may be written as [16]:

$$N_j = k_{j,l}(C_{j,b} - C_{j,int}) = k_{j,g,pore} \left(\frac{p_{j,int} - p_{j,b}}{R_g T} \right) \quad (2)$$

1 where $k_{j,l}$, $k_{j,g,pore}$, $C_{j,int}$, $p_{j,int}$, $C_{j,b}$, $P_{j,b}$, T and R_g denote, respectively the mass transfer
 2 coefficient in the liquid phase for the species j , the mass transfer coefficient in the
 3 hydrophobic membrane for the species j , the interfacial gas concentration in the liquid,
 4 the partial pressure of component j at the interface, the bulk concentration of component
 5 j in the liquid, the bulk partial pressure of component j , the temperature and the
 6 universal gas constant.

7 At the liquid–gas interface, Henry's law is applicable as the solution is dilute [5,11,12]:

$$9 \quad P_{j,int} = P^g_{a,int} = H_a^T [NH_3]_{int} \quad (3)$$

10
 11 here H_a^T is the ammonia's Henry's constant at a given temperature. Taking all this into
 12 account, the overall mass transfer coefficient ($k_{j,ov}$) is given by:

$$14 \quad \frac{1}{k_{j,ov}d_i} = \frac{1}{k_{j,l}d_i} + \frac{R_g T}{H_a^T k_{j,g,pore} b} \quad (4)$$

15
 16 Where negligible resistance in the permeate side is considered and the liquid mass
 17 transfer coefficient for the species j in the lumen side. The mass transport coefficient at
 18 the liquid ($k_{j,l}$) is calculated from Leveque equation under laminar flow condition [5,16]

$$19 \quad k_{j,l} = 1.62 \frac{D_j}{d_i} \left(\frac{d_i^2 \bar{U}}{L D_j} \right)^{1/3} \quad (5)$$

20 Mass transfer coefficient in the hydrophobic membrane for the species j can be written
 21 as [5,12,16]:

$$22 \quad k_{g,pore} = D_{a,c,pore} \left\{ \frac{\varepsilon}{\tau b} \right\} \quad (6)$$

23 where $D_{a,c,pore}$ is the ammonia diffusivity ($m^2 \cdot s^{-1}$), ε is porosity of the membrane, b is
 24 membrane thickness (m) and τ is tortuosity of the pore given by:

$$25 \quad \tau = \frac{1}{\varepsilon^2} \quad (7)$$

26 In hydrophobic membranes the pores are gas filled and the species can be transferred
 27 through the pores mainly by Knudsen or/and viscous flow depending on the ratio
 28 between the membrane pore radius and mean free path of the species. Knudsen
 29 diffusivity can be evaluated from following correlation [16]. The diffusivity of gaseous
 30 ammonia in the pore is calculated by:

$$\frac{1}{D_{a,c,pore}} = \frac{1}{D_{k,a,pore}} + \frac{1}{D_{a,air}} \quad (8)$$

where $D_{k,a,pore}$ is the Knudsen diffusion ($m^2 \cdot s^{-1}$), $D_{a,air}$ is the ammonia diffusivity in the air (m^2/s). The Knudsen diffusion was calculated by:

$$D_{k,a,pore} = \frac{d_{pore}}{3} \left(\frac{8R_g T}{\pi M_a} \right)^{1/2} \quad (9)$$

where d_{pore} is diameter of pore (m), R_g is the universal gas constant ($J \cdot mol^{-1} K^{-1}$), T is the temperature ($^{\circ}K$) and M_a is the molecular weight of ammonia ($g \cdot mol^{-1}$).

On the other hand, for cross-flow hollow-fiber modules (see Figure 3), the hydraulic mean diameter (d_h) can be described as a function of the outer diameter of the central delivery tube (d_D), the shell inner diameter (d_a) and the outer fiber diameter (d_o):

$$d_h = \frac{d_a^2 - d_D^2 - N d_o^2}{N d_o} \quad (10)$$

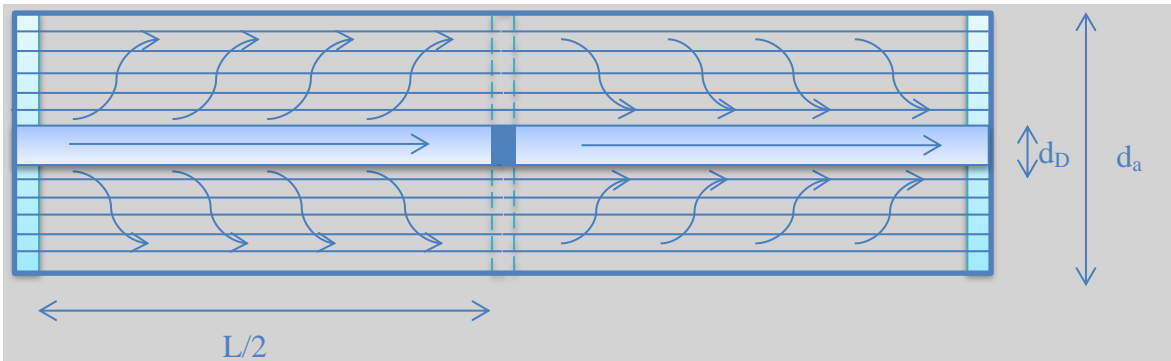


Figure 3. The schematic view of the cross flow hollow fiber module with the velocity profile of flow in the shell side compartment

For those modules most researchers calculate the mean linear velocity (v_{sh}) considering a radial flow pattern

$$v_{sh} = \frac{2Q \ln\left(\frac{d_a}{d_D}\right)}{\pi L (d_a - d_D)} \quad (11)$$

Then the Reynolds number in the shell side (Re_s) is defines as [17]:

$$Re_s = \frac{v_{sh} d_h}{\eta} \quad (12)$$

Table 2 and 3 present the ammonia properties and the hydrophobic membrane specifications respectively.

Table 2. Properties of ammonia at $T = 298 K$

Properties (<i>j</i> is ammonia)	Values
Henry's law constant, H_j (Pa m ³ /mol)	1.62
Diffusivity in water, D_j (m ² /s)	1.76×10^{-9}
Diffusivity in air, $D_{j,air}$ (m ² /s)	1.89×10^{-5}

1

2

Table 3. Specifications of the membrane used in the contactor

Hydrophobic membrane specifications	Values
Pore diameter, d_{pore} (m)	3×10^{-8}
Thickness of the membrane, b (m)	3×10^{-3}
Porosity, ε	0.4
Tortuosity of pore, τ	2.25
Inner diameter of the lumen, d_i (m)	2.4×10^{-4}
Outer diameter of the lumen, d_o (m)	3×10^{-4}
Effective length of the fiber, L (m)	0.15
Number of fibers, N (m)	9950
Shell diameter d_s (m)	0.63
Fiber bundle diameter d_a (m)	0.47
Distribution tube diameter d_D (m)	0.22

3

4

5

6

7

8

In the removal process there is no chemical reaction additionally to the acid base reaction in the lumen side. The symmetry assumed inside the lumen is cylindrical. Furthermore, the radial component of velocity also becomes zero, the rate of diffusion of ammonia in water is negligible and the flow is in the Z direction. Then, the transport equation follows as:

$$\frac{\partial C_j}{\partial t} + U_z \frac{\partial C_j}{\partial z} = D_j \left[\frac{1}{r} \frac{\partial}{\partial r} \left(r \frac{\partial C_j}{\partial r} \right) + \frac{\partial^2 C_j}{\partial z^2} \right] \quad (13)$$

10

11

For the processes carried out under laminar conditions, the velocity profile in the fiber can be written as:

$$U_z(r) = \bar{U} \left\{ 1 - \left(\frac{r}{R} \right)^2 \right\} \quad (14)$$

13

14

where r is radial coordinate (m) and R is radius of the fiber. Defining \bar{U} as the average velocity of the fluid inside the lumen:

$$\bar{U} = \frac{Q}{N\pi R^2} \quad (15)$$

1 where Q is the flow rate (m³/s) and N is the number of fibers in the LLMC. Once
 2 defined the equations for the mass balance within fiber, the boundary conditions are
 3 defined by:

4 **Constant concentration at the inlet of the lumen:**

$$5 \quad C_{j,z=0} = C_0 \quad (16)$$

6 **The boundary condition at the exit of the lumen is defined assuming the diffusion of**
 7 **ammonia to be negligible in comparison to its movement in the same direction of bulk**
 8 **flow,**

$$9 \quad \left(\frac{\partial^2 C_j}{\partial r^2} \right)_{z=L} = 0 \quad (17)$$

10 **In addition, due to the cylindrical shape of the fiber radial symmetry can be defined**
 11 **along its middle point as:**

$$12 \quad \left(\frac{\partial C_j}{\partial r} \right)_{r=0} = 0 \quad (18)$$

13 **Finally, at the inner surface of the hollow fiber, the flux of the ammonia in aqueous**
 14 **phase equals the flux of the gaseous ammonia diffused through the pore [12]:**

$$15 \quad -D_j \left(\frac{\partial C_j}{\partial r} \right)_{r=R} = k_{g,pore} \left(\frac{P_{a,int}^g}{R_g T} \right) \quad (19)$$

16 **Where $P_{a,int}^g$ is the partial pressure of the ammonia at the liquid membrane interface.**

17 **The total ammonium concentration (C_j) (mol·m⁻³) in the aqueous solution is calculated**
 18 **by:**

$$19 \quad C_j = [NH_3] + [NH_4^+] \quad (20)$$

20 **where both concentrations could be estimated by using the acid dissociation constant**
 21 **$K_a(T)$ (NH_4^+/NH_3).**

$$22 \quad K_a(T) = \frac{[NH_3][H^+]}{[NH_4^+]} \quad (21)$$

1 On the other hand, at the liquid (feed phase)-gas (porous phase) interface,
2 Henry's law can be applied:

$$3 \quad P_{a \text{ int}}^g = H_a^T [\text{NH}_3]_{\text{int}} \quad (22)$$

4 $P_{a \text{ int}}^g$ is the partial pressure of the ammonia at the interface, H_a^T is Henry's constant
5 ($\text{Pa} \cdot \text{m}^3/\text{mol}$) and $[\text{NH}_3]_{\text{int}}$ is concentration of ammonia at liquid-gas interface ($\text{mol} \cdot \text{m}^{-3}$).
6 The temperature dependence of $K_a(T)$ and H_a^T could be described by Montes et al. [18]

$$7 \quad K_a(T) = 10^{0.05-2788/T} \quad (23)$$

$$8 \quad H_a^T = \left[\left(\frac{0.2138}{T} \right) * 10^{6.123-1825/T} \right] * R_g T \quad (24)$$

9 **2.3 Numerical simulation**

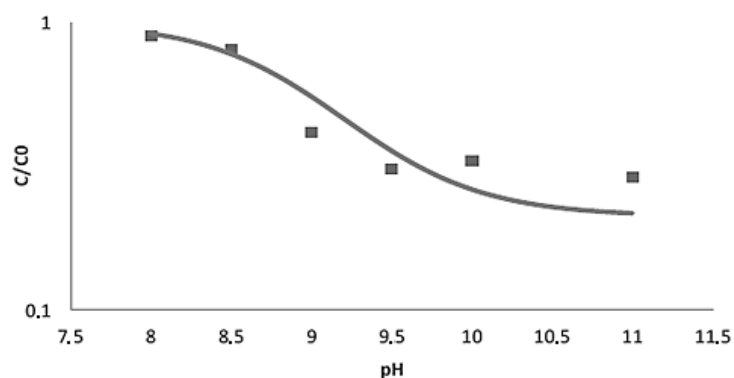
10 On this study the mass transport inside the lumen was simulated using CFD
11 techniques based on finite element method. All the equations related to the separation
12 process with their appropriate boundary conditions were solved using COMSOL
13 Multiphysics version 4.2a. The equations were solved with parallel direct linear solver
14 (PARDISO) with a relative tolerance of 0.001. Under these conditions the solver is well
15 suited for solving stiff and non-stiff non-linear boundary value problems. Adaptive
16 mesh refinement was used to mesh one of the fibers of the LLMC. Furthermore, a
17 refinement on the mesh near to the membrane surface was implemented for all the
18 calculations. A Dell-PC-Intel core 2 (CPU speed is 3 GHz) was used to solve the sets of
19 equations. The mathematical model was developed following the assumptions made by
20 Mandowara and Bhattacharya [12] without taking into account the recirculation in the
21 ammonium solution tank.

22 **3. Results and discussion**

23 **3.1 pH dependence**

24 According to Figure 4, the ammonium removal was clearly affected by the solution pH.
25 The equilibrium between the ammonia gas and ammonium ions depends on the
26 solution's pH, making it the driving force responsible for the separation process. On the
27 same figure, it can be seen within the pH range studied, that the model fits the
28

1 experimental data better at low pH than to at higher. Although the model does not
 2 consider the concentration of ammonia at the shell side, it was not comparable to the
 3 acid concentration. Even in hypothetical cases of comparable concentrations, it has to be
 4 taken into account that the parameter that controls the driven force is the ammonia
 5 partial pressure difference between both sides of the membrane. In order to have effects
 6 on this force, a substantial increase in the pH of the extracting solution must occur to
 7 move the ammonium equilibrium to ammonia gas, which was not the case for none of
 8 experiments carried out. Likewise, the trend predicted by the model follows
 9 qualitatively the tendency of the experimental data and moreover, a turning point is
 10 identified, which coincides with the pKa (pH = 9.3) and is the reaction equilibrium
 11 between ammonium and ammonia. Two different zones are also differentiated in the
 12 plot: one for pH values below the pKa where low values of removal are obtained. The
 13 predominant species is the ammonium and the presence of ammonia is low. The
 14 ammonia is the species that crosses the pores of the membrane and reacts with sulfuric
 15 acid resulting in ammonium sulfate, the minor presence of this species gives rise lower
 16 elimination rates. On the other hand, at pH values above the pKa higher removal
 17 efficiencies are obtained due to the dominant presence of ammonia gas and therefore, a
 18 greater number of molecules of the gas cross the membrane to react with sulfuric acid
 19 resulting in a higher removal performance. A further increase in the pH (> 10) not
 20 represent a significant increase in ammonia removal, that should be taken into account
 21 when designing the real operational conditions in order to save reagents consumption.



22

23 Figure 4. Comparison between the experimental data of concentration at the outlet of
 24 the LLMC (dots) and the profile obtained numerically (line) as function of the pH.

3.2 Initial concentration dependence

Figure 5 shows the results of the experimental data and for removal of ammonium at different initial concentrations of ammonium. It can be observed that the trend of the evolution is similar for the six experiments. Nonetheless, when comparing against the profile obtained numerically differences between them are observed. As can be seen, this error does not have a clear dependence and make think that can be related to errors inherent to the experimental determinations. Accordingly, it can be considered that the removal of ammonium is independent of the initial concentration of the solution to be treated. This is in agreement with the result presented for several authors working in liquid-liquid mode but closed loop regime [12,14,15].

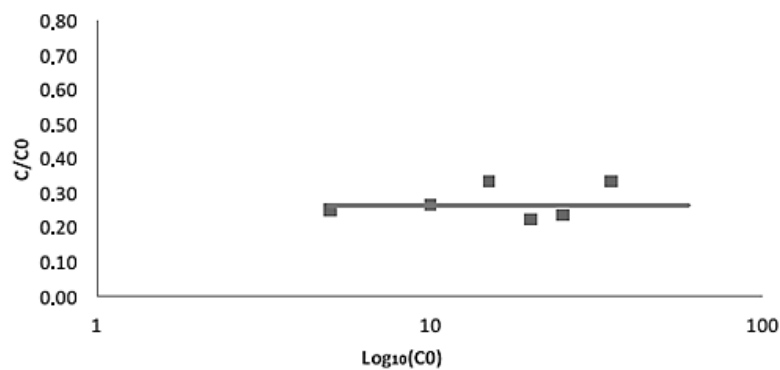


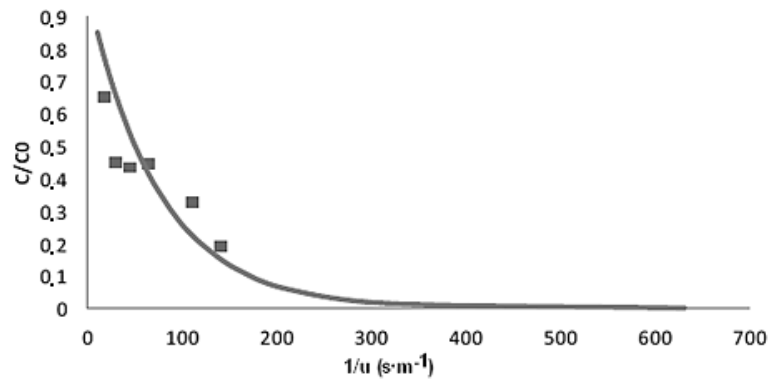
Figure 5. Comparison between the experimental data of concentration at the outlet of the LLMC (dots) and the profile obtained numerically (line) as function of the initial concentration of ammonium, C_0 ($\text{mg}\cdot\text{L}^{-1}$).

3.3 Flow rate dependence

The other important parameter to be taken into account is the flow rate which affects the residence time of the solution inside the LLMC; the larger the flow rates the lower the efficiency of the contactor (see Figure 6). For each experiment, its respective linear velocity (U) was calculated by means of Equation 15 and the results are presented as function of the reciprocal velocity ($1/U$).

According to Figure 6, the model is substantially consistent with the experimental data. However, the fact that both are not identical can be attributed again to experimental error, such as the presence of any air bubbles in the circuit, the error in the ammonia selective electrode, among others. It can be seen, that at low values of $1/U$ (at high flows) lower removal is reached. Additionally it can be seen that the profile presents a

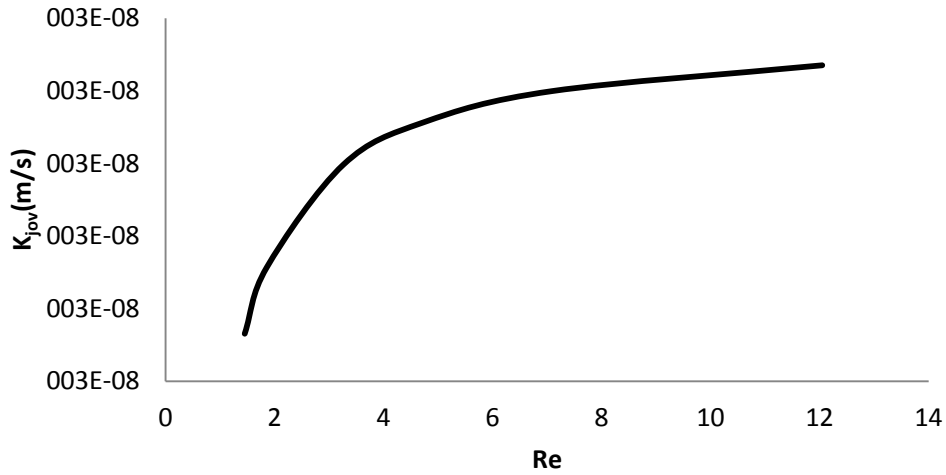
- 1 zones in which a small change in flow results in a large variation in ammonia removal.
 2 Nevertheless, it has to be taken in to account that very low flow rates may produce an
 3 extra resistance in the liquid phase.
 4 This behavior is in concordance with the values reported in a previous work [5]



- 5
 6 Figure 6. Comparison between the experimental data of concentration at the outlet of
 7 the LLMC (dots) and the profile obtained numerically (line) as function of the initial
 8 concentration of ammonium, C_0 ($mg \cdot L^{-1}$)

9 3.4 Mass transport coefficient calculation

- 10 From equation 4 the overall mass transport coefficient can be calculated for each flow
 11 defined in the experimental part (Table 1). Figure 7 shows how this coefficient is almost
 12 independent to Reynolds numbers (in the lumen) larger than 6. Nevertheless the
 13 variation in the complete range is just about 1.5%. Calculated values of various
 14 parameters from the model equations are given in Table 4. In all the experiments, the
 15 flow can be consider laminar at both sides of the membrane due to the low values for
 16 their respective Reynolds numbers obtained with equation 12 (Table 1).



1
2 Figure 7. Overall mass transport coefficient as function of the Reynolds number in the
3 lumen

4
5 Table 4. Calculated values of various parameters from the model equations

Parameter	Value
Mass transfer coefficient in the hydrophobic membrane for $\text{NH}_{3(g)}$, $k_{j,g,pore}$ (m/s)	4.06×10^{-4}
Knudsen diffusivity, $D_{k,i,pore}$ (m^2/s)	1.92×10^{-7}
Combined diffusivity, $D_{j,c,pore}$ (m^2/s)	1.90×10^{-7}

6
7 Table 5. Reynolds numbers in the lumen (Re) and the shell side (Re_s)

Q ($\text{m}^3 \cdot \text{s}^{-1}$) $\times 10^6$	Re	Re_s
2.72	1.45	2.01
3.48	1.85	2.57
6.12	3.26	4.53
8.86	4.72	6.56
1.33	7.09	9.85
2.26	12.04	16.74

8
9 In order to generalize the results of this study, the following dimensionless variables are
10 introduced:

$$11 \quad \xi = \frac{2r}{d_i}; \quad \zeta = \frac{z}{L}; \quad \check{C} = \frac{c}{c_0} \quad (25)$$

12 With the use of these new variables and after simplification at the steady state the
13 transport equation and its boundary conditions result in:

$$15 \quad \frac{\partial \check{C}}{\partial \zeta} = 2 \left(\frac{DL}{vd_i^2} \right) \left[\left(\frac{1}{1-\xi^2} \right) \left\{ \frac{1}{\xi} \frac{\partial}{\partial \xi} \left(\xi \frac{\partial \check{C}}{\partial \xi} \right) \right\} \right] \quad (26)$$

$$\check{C}_{\xi=0} = 1; \frac{\partial^2 \check{C}}{\partial \xi^2} \Big|_{\xi=1} = 0; \frac{\partial \check{C}}{\partial \xi} \Big|_{\xi=0} = 0; \frac{\partial \check{C}}{\partial \xi} \Big|_{\xi=1} = -\frac{Sh}{2} \check{C}_{\xi=1} \quad (27)$$

where the coefficient $Sh = \frac{k_{g,pore} d_i}{D_j} = 55.4$ is the Sherwood number and the term $\frac{V d_i^2}{DL}$ is the dimensionless Graetz number based on the internal fiber diameter, which is related to the Reynolds and Schmidt numbers as $Gr = \frac{Re Sc di}{L}$. The Sherwood number represents the ratio of convective to diffusive mass transport. According to value obtained in this study, the mass transport occurring in the boundary was carried out mainly by convective transport instead of molecular diffusion. On the other hand, when the definition of the Sherwood number is changed to $\frac{k_{g,pore} d_i}{D_{a,c,pore}}$, the obtained value of xxx is lower than 1. The combined diffusivity in the pore ($D_{a,c,pore}$) takes into account the effects of the Knudsen diffusion and the value near to the unity in the new definition of the Sherwood number, which means that the Knudsen diffusion is the responsible of the mass transport in the membrane pore. These results are in agreement with values reported in literature [12].

3.5 Number of modules

Taking into account all the results, it can be said that when the pH values promote a high concentration of ammonia and the flow rate maintain an adequate residence time, the LLMC will remove the same percentage of the ammonium from the feeding solution when working in open loop configuration irrespective of the feed concentration.

The fraction of ammonia at the end of a single contactor can be defined as:

$$X^* = \frac{C}{C_0} \quad (28)$$

Accordingly, when placing N_m number of LLMC in series the resultant concentration can be expressed through:

$$C = C_0 X^{*Nm} \quad (29)$$

Therefore, the number of modules to be used to reach a given concentration can be calculated from such simple expression:

$$N_m = \frac{\log\left(\frac{C^*}{C_0}\right)}{\log(X^*)} \quad (30)$$

Where C^* is the desirable concentration.

For instance the value of X^* obtained from experiments with pH of 10 and flow rate of feed of $3.48 \times 10^{-6} \text{ m}^3 \cdot \text{s}^{-1}$ was nearly 0.3 for experimental data. Figure 8 shows the ammonia concentration against number of modules (N_m) in series and it is observed that removal efficiency can be larger to 95% with three modules.

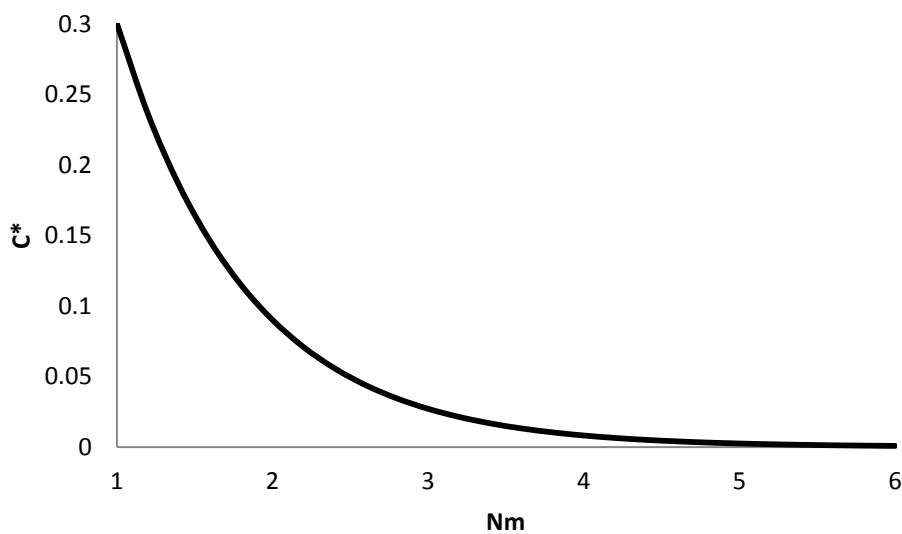


Figure 8. Ammonia concentration at the outlet of the series of contactors as function of the number of modules

4. Conclusions

In view of the results of this study, the technology of LLMC's operating in open loop configuration is potentially suitable to remove water with low levels of ammonium. The effect of the feed stream pH, initial concentration of ammonium and flow rate was thoroughly studied in order to describe its influence during the removal process and it was determined a simple expression to estimate the number of membrane modules placed in series necessary to reach a given target value. The maximum efficiency experimentally observed for single step was 78% under feed values of pH, initial concentration and flow rate of 10, $2.72 \times 10^{-6} \text{ m}^3 \cdot \text{s}^{-1}$ and $15 \text{ mg} \cdot \text{L}^{-1}$ respectively.

1 Furthermore, it is demonstrated experimentally and numerically that the ammonium
2 removal efficiency in LLMC operating in open loop configuration is improved by
3 raising the pH and decreasing the flow rate. Accordingly, the model purposed in this
4 study can describe properly the experimental data and can be used to evaluate and
5 design the ammonia removal process by LLMC.s.

6 **List of symbols:**

- 7 A membrane surface area (m^2)
8 b is membrane thickness (m)
9 C^* desirable concentration at the outlet of the modules ($\text{mol}\cdot\text{m}^{-3}$)
10 C_j the total ammonium concentration in the feed phase ($\text{mol}\cdot\text{m}^{-3}$)
11 C_0 is the inlet concentration ($\text{mol}\cdot\text{m}^{-3}$)
12 $D_{a,\text{air}}$ is the ammonia diffusivity in the air ($\text{m}^2\cdot\text{s}^{-1}$)
13 $D_{a,c,\text{pore}}$ is the ammonia diffusivity ($\text{m}^2\cdot\text{s}^{-1}$),
14 D_j diffusivity of the component j in water ($\text{m}^2\cdot\text{s}^{-1}$)
15 $D_{k,a,\text{pore}}$ is the Knudsen diffusion ($\text{m}^2\cdot\text{s}^{-1}$)
16 d_{pore} is diameter of pore (m)
17 H_a^T is Henry's constant ($\text{Pa}\cdot\text{m}^3\cdot\text{mol}^{-1}$)
18 K_a ammonium acid dissociation constant
19 $K_{g,\text{pore}}$ the mass transfer coefficient inside the pore ($\text{m}\cdot\text{s}^{-1}$)
20 L length of the hollow fibers (m)
21 M_a is the molecular weight of ammonia ($\text{g}\cdot\text{mol}^{-1}$)
22 N is the number of fibers in the HFMC
23 Nm number of modules
24 $[\text{NH}_3]$ concentrations of ammonia ($\text{mol}\cdot\text{m}^{-3}$)
25 $[\text{NH}_3(\text{g})]$ concentration of ammonia gas ($\text{mol}\cdot\text{L}^{-1}$)
26 $[\text{NH}_4^+]$ concentrations of ammonium in the feed solution ($\text{mol}\cdot\text{m}^{-3}$)
27 $P_{a,\text{int}}^g$ is the partial pressure of the ammonia at the interface (Pa)
28 Q is the flow rate (m^3/s)
29 R radius of the fiber (m)
30 r radial coordinate (m)
31 R_g is the universal gas constant ($\text{J}\cdot\text{mol}^{-1}\cdot\text{K}^{-1}$),
32 T is the temperature (K)
33 U the velocity ($\text{m}\cdot\text{s}^{-1}$)

- 1 \bar{u} average velocity($\text{m}\cdot\text{s}^{-1}$)
 2 V volume (m^3)
 3 X* fraction obtained with one module
 4 z axial coordinate (m)
 5 ε is porosity of the membrane,
 6 τ is tortuosity

7 **Acknowledgements**

8 This study has been supported by the ZERODISCHARGE project (CPQ2011-26799)
 9 financed by “Ministerio de Economía y Competitividad” and the Catalan government
 10 (project ref. 2009SGR905). The authors also thank to A. Gali, E. Larrotcha and E.
 11 Marzo, project leaders of the Greenlysis project from CETAQUA, for their support and
 12 help on the study.

13 **5. References**

- 14 [1] A. Ursua, L.M. Gandia, P. Sanchis, Hydrogen Production From Water
 15 Electrolysis: Current Status and Future Trends, Proc. IEEE. 100 (2012) 410–426.
- 16 [2] E. Marzo, A. Gali, B. Lefevre, L. Bouchy, A. Vidal, J.L. Cortina, et al.,
 17 Hydrogen and Oxygen Production using Wastewater Effluent Treated with Ultra-
 18 Filtration and Membrane Distillation (Greenlysis), Procedia Eng. 44 (2012)
 19 1744–1746.
- 20 [3] P. Peng, A.G. Fane, X. Li, Desalination by membrane distillation adopting a
 21 hydrophilic membrane, Desalination. 173 (2005) 45–54.
- 22 [4] S.N. Ashrafizadeh, Z. Khorasani, Ammonia removal from aqueous solutions
 23 using hollow-fiber membrane contactors, Chem. Eng. J. 162 (2010) 242–249.
- 24 [5] A. Mandowara, P.K. Bhattacharya, Membrane contactor as degasser operated
 25 under vacuum for ammonia removal from water: A numerical simulation of mass
 26 transfer under laminar flow conditions, Comput. Chem. Eng. 33 (2009) 1123–
 27 1131.
- 28 [6] Z. Xie, T. Duong, M. Hoang, C. Nguyen, B. Bolto, Ammonia removal by sweep
 29 gas membrane distillation., Water Res. 43 (2009) 1693–9.
- 30 [7] Z. Ding, L. Liu, Z. Li, R. Ma, Z. Yang, Experimental study of ammonia removal
 31 from water by membrane distillation (MD): The comparison of three
 32 configurations, J. Memb. Sci. 286 (2006) 93–103.

- 1 [8] M.S. EL-Bourawi, M. Khayet, R. Ma, Z. Ding, Z. Li, X. Zhang, Application of
2 vacuum membrane distillation for ammonia removal, *J. Memb. Sci.* 301 (2007)
3 200–209.
- 4 [9] M.J. Semmens, D.M. Foster, E.L. Cussler, Ammonia removal from water using
5 microporous hollow fibers, *J. Memb. Sci.* 51 (1990) 127–140.
- 6 [10] S.R. Wickramasinghe, M.J. Semmens, E.L. Cussler, Mass transfer in various
7 hollow fiber geometries, *J. Memb. Sci.* 69 (1992) 235–250.
- 8 [11] X. Tan, S.P. Tan, W.K. Teo, K. Li, Polyvinylidene fluoride (PVDF) hollow fibre
9 membranes for ammonia removal from water, *J. Memb. Sci.* 271 (2006) 59–68.
- 10 [12] A. Mandowara, P.K. Bhattacharya, Simulation studies of ammonia removal from
11 water in a membrane contactor under liquid-liquid extraction mode., *J. Environ.*
12 *Manage.* 92 (2011) 121–30.
- 13 [13] G.K. Agrahari, S.K. Shukla, N. Verma, P.K. Bhattacharya, Model prediction and
14 experimental studies on the removal of dissolved NH₃ from water applying
15 hollow fiber membrane contactor, *J. Memb. Sci.* 390-391 (2012) 164–174.
- 16 [14] M. Rezakazemi, S. Shirazian, S.N. Ashrafizadeh, Simulation of ammonia
17 removal from industrial wastewater streams by means of a hollow-fiber
18 membrane contactor, *Desalination.* 285 (2012) 383–392.
- 19 [15] F. Nosratinia, M. Ghadiri, H. Ghahremani, Mathematical modeling and
20 numerical simulation of ammonia removal from wastewaters using membrane
21 contactors, *J. Ind. Eng. Chem.* (2013).
- 22 [16] E. Drioli, A. Criscuoli, E. Curcio, *Membrane contactors: Fundamentals,*
23 *applications and potentialities*, 2006.
- 24 [17] S. Shen, S.E. Kentish, G.W. Stevens, Shell-Side Mass-Transfer Performance in
25 Hollow-Fiber Membrane Contactors, *Solvent Extr. Ion Exch.* 28 (2010) 817–844.
- 26 [18] F. Montes, C.A. Rotz, H. Chaoui, Process Modeling of Ammonia Volatilization
27 from Ammonium Solution and Manure Surfaces: a Review with Recommended
28 Models, *Trans. Asabe.* 52 (2009) 1707–1719.

29